ORIGINAL ARTICLE

Microemulsions for remediation of light non-aqueous-phase liquids in aquifer rocks

Letícia Alonso Bernardez[1] · Luiz Rogério Pinho de Andrade Lima[1]

Abstract

In this study, the formulation of microemulsions as cleaning systems is studied using model hydrocarbons to simulate light non-aqueous-phase liquids (LNAPL). The effects of the type of surfactant, the size of the LNAPL compound chain, the type of co-surfactant, salinity, pH, and temperature on the phase behavior of LNAPL-water-surfactant were investigated. Using pseudo-ternary diagrams, the effects of these variables on the microemulsion domain size were analyzed. The results show that choosing a co-surfactant with a shorter carbon chain length significantly increases the microemulsion domain. The microemulsion domain increases with the decrease in the length of the LNAPL compounds. Decreasing the salinity, pH or temperature increased the microemulsion domains. A sandstone core flooding experiment was carried out using kerosene as LNAPL and solution of Triton X-100 or LAS/iso-amyl alcohol as surfactant/co-surfactant. The results of the flooding experiment with low concentration of surfactant showed a total recovery of 50% of LNAPL by 14 bed volumes (7 of water and 7 of the Triton X-100/iso-amyl alcohol and 60% of the LNAPL by analogous injection of LAS/iso-amyl alcohol. The results of the flooding experiment with high concentration of surfactant showed a recovery of 67% of the LNAPL by 3 bed volumes of water injection and an extra 36% by 2 bed volumes of the surfactant/co-surfactant solution injection. This shows the strong effect of the microemulsion in the mobilization of the residual LNAPL from an aquifer rock using an appropriate formulation of surfactant solutions.

Keywords Site remediation · Microemulsion · Phase equilibrium · Sandstone · LNAPL

Introduction

The use of the microemulsion technique has received some attention in recent years as a remediation method for non-aqueous-phase liquid (NAPL) contaminated soils and aquifer rocks (Martel et al. 1993; Bernardez et al. 2009; Li et al. 2011, 2014; Bernardez and de Andrade Lima 2014; Javanbakht and Goual 2016; Javanbakht et al. 2017). It is recognized that the mobilization of the NAPL is due to the reduction of the interfacial tension NAPL/water and the phase behavior of surfactant-aqueous-phase/NAPL systems is a key factor in interpreting the performance of NAPL recovery by microemulsion (Ceglie et al. 1987; Kegel and Lekkerkerker 1993; Bayrak and Isca 2005).

✉ Luiz Rogério Pinho de Andrade Lima
lelo@ufba.br

1 Departament of Materials Science and Technology, Federal University of Bahia, Rua Aristides Novis, n.2, Salvador, BA 40210-630, Brazil

Investigations into systems containing three components (oil-phase, water, and surfactant) make use of geometrical representation. However, with the introduction of a fourth component to the system (co-surfactant), it is more convenient to use plane representations, such as the triangular ternary diagrams, known as pseudo-ternary. One of the tops of the triangle then represents the mixture of surfactant and co-surfactant. The second top represents the aqueous phase and the last top consists of the oil phase. Triangular pseudo-ternary-phase diagrams are tetrahedron cuts characterized by a fixed co-surfactant/surfactant mass ratio so that the apices were oil, water, or brine (a pseudo-component) and the surfactant-co-surfactant mixture (Bernardez and de Andrade Lima 2014).

The optimum formulation of microemulsions can be obtained by analyzing the phase behavior of the oil phase–water–surfactant system and the effect of the salinity, the nature of the NAPL components, the type of surfactant and co-surfactant, and the temperature, among other variables (Salager et al. 1979; Bellocq et al. 1980;

Voca et al. 1988; Xu et al. 2001; Bayral and Iscan 2005; Azira and Tazerouti 2007; Azira et al. 2008; Jin et al. 2016). The importance of the contributions of the components in the microemulsions, in general, follows the order: co-surfactant > oil phase > surfactant (Ceglie et al. 1987; Kahlweit et al. 1991; Keger and Lekkerkerker 1993).

Industrial surfactant systems with light non-aqueous-phase liquids (LNAPLs), which have received less attention in previous works, are the focus of this study. In the first part of this study, pseudo-ternary-phase diagrams for water/LNAPL/surfactants-co-surfactant are developed, and the effects of the type of surfactant, co-surfactant, salt, pH and temperature on the microemulsion zone are addressed. Hexane was used as model of a LNAPL. In the second part, the study evaluates the performance of the formulation of microemulsions as cleaning systems to clean light non-aqueous phase liquids (LNAPLs) from the Botucatu Formation (Brazil) as the aquifer rock. Experimental core flooding tests with different types of surfactant were performed to compare the recovery efficiency. Kerosene was used in the flooding experiments performed in a plug of sandstone. These LNAPLs were used a surrogate for complex multicomponent NAPLs, such as the petroleum of Bahia, Brazil, which is essentially composed of light alkanes (between C_{12} and C_{16}) and paraffin (between C_{16} and C_{30}).

This research attempts to improve the understanding of the recovery of LNAPLs using microemulsion solutions and the factors that control it. The results may provide a rational basis for selecting the optimum formulation and conditions for LNAPLs recovery from porous medium. The knowledge gained may lead to strategies to significantly enhance recovery rates when surfactant-aided remediation is applied.

Materials and methods

Chemicals

The chemicals used to prepare the microemulsion systems were: Triton X-100 (Vetec) and linear alkylbenzene sulfonate (LAS, provided by the Deten Quimica S/A). The co-surfactants were iso-amyl alcohol (Vetec) and n-butanol (Vetec). As LNAPL hexane (Sigma Aldrich), dodecane (Sigma Aldrich), and commercial aromatic free kerosene (Cedep) were used. Synthetic brines were aqueous solutions of sodium chloride (Quimex) in distilled water.

The present study focuses on the use of both types of surfactants (sulfonate and Triton X-100) in soil and aquifer rock LNAPL remediation. The petroleum sulfonates were chosen due to their low cost, low adsorption at neutral to high pH in the porous medium and their effects on the interfacial tension. Sulfonates are ionic surfactants used in several fields including the oil recovery industry (Sanz and Pope

1995; Iglauera et al. 2009; Jeirani et al. 2014; Demirbas et al. 2015). The surfactant LAS is one of the most extensively studied anionic surfactants (Bera and Mandal 2014). However, non-ionic surfactants, such as Triton X-100 (iso-octylphenyl ether), are commonly used in numerous commercial and industrial products. In addition, Triton X-100 is one of the most commonly used surfactants in experimental studies on solubilization and biodegradation of hydrophobic organic compounds (Voca et al. 1988; Bayrak and Iscan 2005; Azira and Tazerouti 2007; Azira et al. 2008).

Figure 1a and b show the molecular structure of linear alkylbenzene sulfonate (LAS) and Triton X-100. The number of carbon atoms in the chain of LAS varies between 10 and 14. Triton X-100 has a carbonic chain ranging from 9 to 10 carbon atoms from one side of the oxygen atom and 15 carbon atoms, including a benzene ring, on the opposite side.

Phase diagram of LNAPL-water-surfactant/ co-surfactant systems

The range of formation of the microemulsion domain is determined especially by the physico-chemical properties of the oil phase, aqueous phase, and surfactant with some essential conditions required for the formation of the microemulsion. These include the existence of a very low interfacial tension at the oil–water interface. The effects of the surfactant and the co-surfactant type and the oil carbon chain lengths on the interfacial tension (LNAPL-water) were assessed. The measurements were made using a tensiometer Sigma 702 (Biolin Scientific AB, Sweden), the du
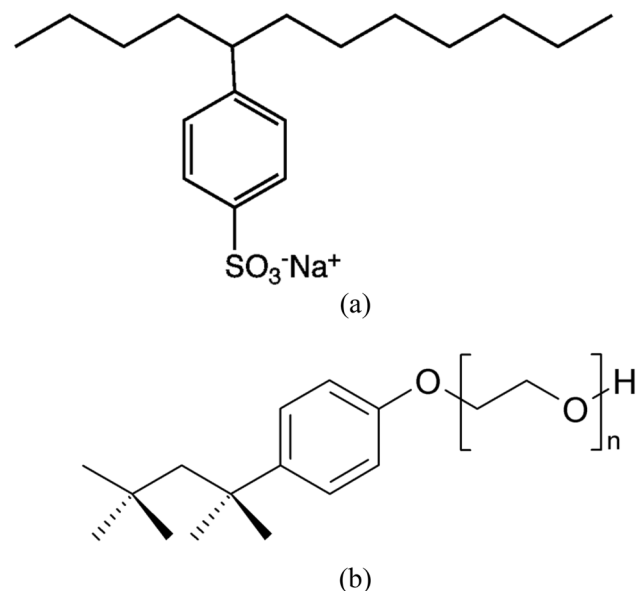
Fig. 1 Molecular structure of surface-active agents **a** linear alkyl benzene sulfonate (LAS) and **b** Triton X-100 ($n = 9$–10)

Noüy ring method, and corrector factors by Huh and Mason (1975). The samples were prepared with solutions of water/surfactant and hydrocarbons.

The presence of microemulsion (one phase) domains for the studied systems was determined using glass centrifuge tubes of 15 mL and a solution of specific volumes, using burettes. These tubes were previously cleaned using Extran (Merk) and abundant distilled water, then washed with ethylic alcohol, then washed using acetone, and dried in an oven. The specific volumes of water, the surfactant and co-surfactant solution, and a total of 10 mL NALP (hexane, dodecane, or kerosene) were put inside the centrifuge tubes and homogenized under stirring. After resting for a few minutes, the tube was centrifuged at about 3000 rpm for 10 min. After that, the presence of one or more phases was observed and the data (composition and number of phases) were used to draw the phase diagrams. The surfactant/co-surfactant ratio was kept constant (at 1:2) for the systems.

The pseudo-ternary phase diagrams were built by plotting the amounts of water, oil, and co-surfactant/surfactant phases used in each experiment (Azira and Tazerouti 2007; Azira et al. 2008; Bernardez and de Andrade Lima 2014). After constructing the pseudo-ternary phase diagrams featuring the microemulsion domains of interest, one point with a specific composition was chosen inside each microemulsion domain in the diagrams. The microemulsion systems were then homogenized under stirring and centrifuged. The visual observation of macroscopic properties of the samples enabled the identification of the boundaries between microemulsion (homogeneous) and multi-phase domains.

LNALP mobilization in porous media

Characterization of the porous media

The porous media used in this study are samples from the Botucatu Formation (Brazil) (Bigarella and Salamuni 1967). These are quartzitic sandstone, fine-textured, well-sorted without pebbles (see Fig. 2) (Correa et al. 2019). Core samples of 3.8 cm (1 ½ in) in diameter and 20.0 cm long were put inside PVC tubes of 5.08 cm (2 in) (external diameter). Two acrylic plate distributors were attached to the edges of the core porous bed, featuring two ends connected to the injection and the discharge lines. After this, the core sample was fixed inside the PVC tube using an epoxy resin. Figure 3a shows the core sample mounted in a system that uses a constant-flow high-performance liquid chromatography (HPLC) piston pump (Series I Pump, Cole-Parmer) to determine the core permeability and porosity.

To determine the porosity or void fraction of the porous bed, it was previously weighed using a semi-analytical balance. Using a HPLC pump, distilled water was injected at a constant flow, then it was weighed again (Fig. 3a). The
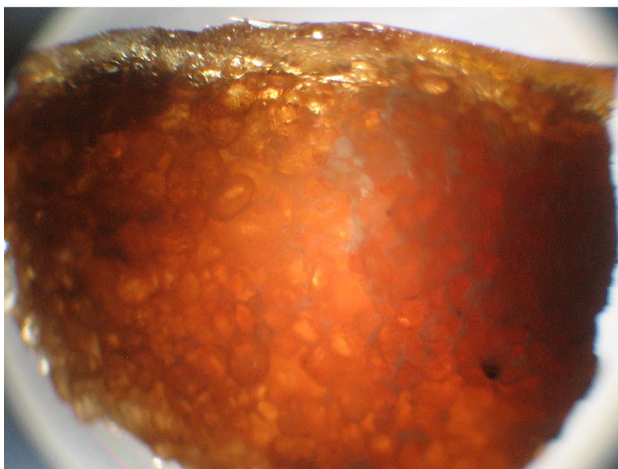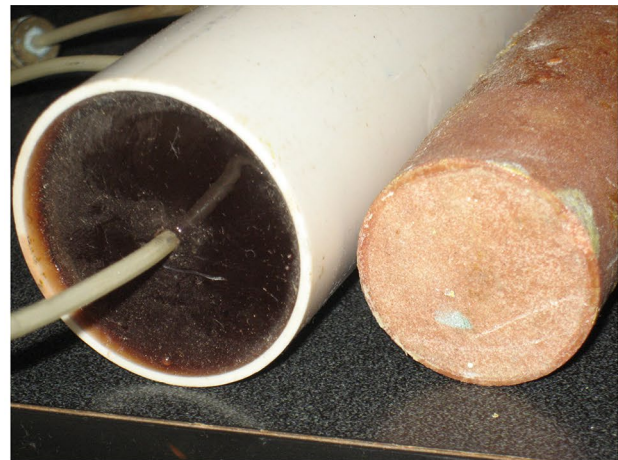
Fig. 2 Details of the Botucatu sandstone core used in the experiments

difference in weights indicates the amount of the water in the porous bed, and as it was saturated, the volume occupied by the water is approximately the volume of the pores of the core sample. The bed porosity (ε) is the ratio between the pore volumes by the total volume of the porous bed and is given by the following expression:

Fig. 3 **a** System used in the permeability experiments. **b** System used in the core flooding experiments. **c** Schematic representation of the experimental setup used in the sandstone core samples residence time distribution tests. The numbers stand for: (1) Distilled water or sulfuric acid reservoir, (2) HPLC pump, (3) Liquid injection in the bed, (4) Solid bed, (5) Solution exit and small tank with a hole in the bottom, (6) Waste solution reservoir, (7) pH electrode, (8) pH meter, and (9) Personal computer

(a)

(b)
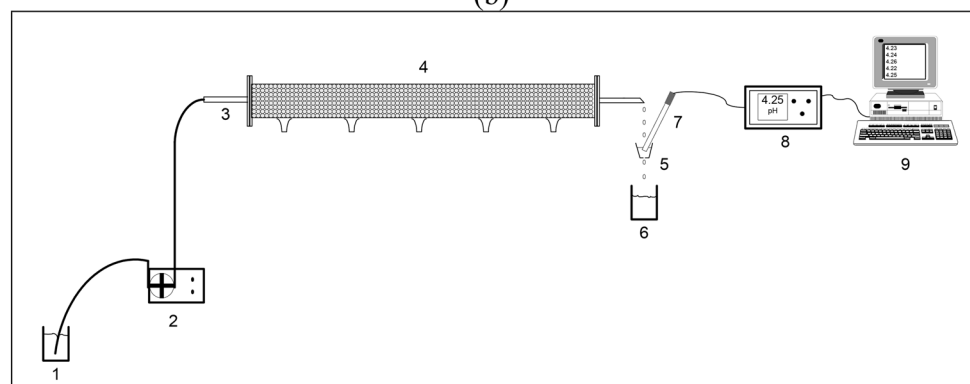
(c)

$$\varepsilon = \frac{V_w}{V_t} \tag{1}$$

where V_w is the volume of void space or volume of water in the porous bed and V_t is the total bed volume.

The permeability of the porous media can be estimated using a constant flow and measuring the pressure drop of water. The classical Darcy equation can be used to estimate this important property of the porous media (Kameda 2005; Correa et al. 2019):

$$\frac{q}{A} = \frac{k}{\mu} \frac{\Delta P}{L} \tag{2}$$

where q is the volumetric flow rate, A is the total cross-sectional area of the porous bed, μ is the fluid viscosity, ΔP is the pressure drop, L is the sample length, and k is the absolute permeability of the rock. In the present case, the core samples and a constant flowrate HPLC pump were used (Fig. 3a). The core sample was first saturated with water at a low flow rate, then the flow rate was progressively changed to high values and the pressure drop was observed throughout the experiment. By plotting the water flux (q/A) versus the pressure gradient ($\Delta P/L$), it is possible to confirm the Darcy flow in the porous media. The slope of the straight line gives k/ε and enables the estimation of the absolute permeability (k) of the porous media.

To characterize the internal pore structure of the Botucatu sandstone, tracer tests were carried out using a core sample and a miscible tracer (de Andrade Lima 2006; Bernardez et al. 2008). Water was inserted into the core sample by an HPLC constant flow pump; concentrated sulfuric acid (98%) with a food red dye was used as a tracer. A volume of 3 mL of the tracer was used in the tests. The tracer impulsions were carried out by changing the pump feed tube from the water to the acid reservoir. The red dye color was used to visualize the path of the acid in the polyethylene tubes and to indicate the time that the acid goes in the core samples. The pregnant solution was collected in a small reservoir with a small hole in the bottom, which retained a small volume of the solution and enabled pH measurement by the electrode. The measured pH as a function of the time was tracked on a PC using the RS-232 interface and this was used to perform the subsequent analysis. After each experiment, the bed was continuously rinsed with water until a pH of about 7 to ensure that the tracer was removed. All experiments were conducted at room temperature. The tracer tests were performed for liquid flow rates of 2.75 and 4.40 mL/min. The first test was performed with significant residual NAPL in the core sample, and the other tests were performed after core clean-up using a commercial surfactant solution and ethylic alcohol, and after rinsing for 3 h with water. In the present case, the measured tracer concentration is given by the concentration of hydrogen ion ($[H^+] = 10^{-pH}$).

LNAPL porous media mobilization

The mobilization of the LNAPL from the porous media was performed using a modification of the apparatus described above. The system for the fluid injection at constant flow rate is composed of an HPLC pump, which acts as a hydraulic drive for a 250 mL stainless steel syringe with a Teflon plunger for the fluid injection (Fig. 3b). The core sample discharge was collected in a measuring cylinder. The injection flow rate in the present study was fixed at 2.0 or 2.75 mL/min. Kerosene was used in the porous bed floods due to its similarities to the properties of crude oil high in paraffin (C_{18} to C_{30}).

The nominal retention time of the water in the sample core (τ) is given by the ratio between the core void volume or water volume (V_w) and the water flow rate (Q_w):

$$\tau = \frac{V_w}{Q_w} \tag{3}$$

This value can be used to record the evolution of the dynamic flooding experiments as a function of the bed volume of water (BV) instead of the experiment time (t), as follows:

$$BV = \frac{t}{\tau} \tag{4}$$

Before the flooding tests, the sample core was saturated with kerosene by pumping about 150 mL of this through the core. Due the fact that the bed volume was about 11 ml, it gives about 10 bed volumes. The LNAPL recovery tests were performed in two steps. In the first one, only direct displacement of the oil by 7 bed volumes of water (BV) was performed. The second one used 7 bed volumes of microemulsion (surfactant/co-surfactant water solution) displacement to recover the oil remaining in the porous bed. The solutions used in the experiments were based on the previously determined phase diagrams. In the first test, a low concentration of the surfactant Triton X-100 or LAS and iso-amyl alcohol was used. The surfactant-co-surfactant mixture/water with ratio 1:1000 and a surfactant/co-surfactant ratio of 2:1 or 1:2 was used in the test. The second test used a high concentration of the surfactant. The composition of the surfactant (LAS)-co-surfactant (iso-amyl alcohol) mixture/water used was a 5.7:1 ratio with a surfactant/co-surfactant ratio of 2:1. All the collected samples of the drained liquid were centrifuged. The LNAPL recovery was calculated taking into account the core total pore volume and the collected volume of LNAPL as a function of time.

Results and discussion

Phase diagram of LNAPL-water-surfactant/co-surfactant systems

The interfacial tension for the water–hexane system is reduced from 42.36 to 12.9 mN/m by the addition of alcohol. By adding Triton X-100, the interfacial tension water–hexane system is reduced from 11.99 to 2.23 mN/m (Table 1). The interfacial tension between water and the alkane compounds decreases when the chain length of alkane used increases (hexane/water is 42.36, dodecane/water is 34.95, and kerosene/water is 23.54 mN/m) (Table 1). The interfacial tension hexane/water decreases from 42.35 to 26.51 when the pH moves from 6 to 3. The interfacial tension of kerosene/water decreases with the use of a sulfonate surfactant/co-surfactant (Table 1). The use of LAS and alcohol decreases the interfacial tension hexane/water and kerosene/water dramatically, which enables the mobilization of NAPL.

The addition of a co-surfactant leads to a further reduction in the interfacial tension and fluidizes the interfacial surfactant film, which can expand the domain of existence of the microemulsion system. It has been shown that co-surfactants reduce gel formation, microemulsion viscosity, and microemulsion equilibration time (Kahlweit et al. 1991; Bera and Mondal 2014). The formation and the physico-chemical properties of microemulsions are influenced by the presence of alcohol and by the length of their hydrocarbon chain (Ceglie et al. 1987; Keger and Lekkerkerker 1993). The length of the chain interferes with the structure and size of the microemulsion domain. The co-surfactants used in the non-ionic and ionic systems are the medium-chain-length alcohols iso-amyl alcohol (3-methylbutan-1-ol) and n-butanol, which produce bi-continuous microemulsion over a wide range of concentrations. Longer-chain alcohols favor the formation of a liquid crystal phase, and the shorter-chain alcohols are too soluble in the aqueous phase and are therefore ineffective as co-surfactants.

**Table 1** Interfacial tension for LNAPL-water systems

System:	(mN/m)
Hexane/Water	42.36
Hexane/Water (pH = 3)	26.51
Dodecane/Water	34.95
Kerosene/Water	23.54
Hexane/Water/Iso-amyl alcohol	12.90
Hexane/Water/Iso-amyl alcohol-Triton X-100	2.23
Hexane/Water/ Iso-amyl alcohol-LAS	≈0.00
Kerosene/Water/ Iso-amyl alcohol l-LAS	1.75

The influence of the co-surfactants iso-amyl alcohol and n-butanol on the formation of microemulsions was investigated at a ratio of (1:2) for the system Triton X-100/co-surfactant/water/hexane. Pseudo-ternary-phase diagrams were constructed to determine the microemulsion domain (Fig. 4a). Figure 4b shows the effect of two different co-surfactants on the microemulsion domain. It can be seen that the use of n-butanol provides better results than the use of iso-amyl alcohol. The microemulsion domains are larger when alcohols of a shorter-chain length are used. The n-butanol has a shorter hydrocarbonic chain and iso-amyl alcohol has a branched and longer carbonic chain, which can favor the microemulsion region.

The main property interest of microemulsions is to associate two liquids of different polarities, and the role of ionic strength of the solution on the microemulsion structure is critical. It is therefore important to know the effect of salinity on the formation and microemulsion domains. To study the effect of the ionic strength, solutions of 1 and 3 mol/L of sodium chloride were used. As can be seen in Fig. 4c, the domain of the microemulsion decreases when the amount of salt in the system increases. This can be attributed to the fact that the increasing concentration of lyotropic salts, such as NaCl, decreases the mutual solubility between H_2O and the non-ionic surfactant. It has been reported that the phase diagram of ternary systems composed of a non-ionic surfactant, water, and oil changed with the amounts and types of salts added to the water.

The variation in the pH of the aqueous phase modifies the characteristics of adsorption on the surface of the adsorbent and the degree of ionization of the surfactant. The influence of the pH on the formation and existence of the microemulsion for the system with the two surfactants was studied.

Figure 4d shows the influence of pH on the microemulsion domain for a system containing non-ionic surfactant Triton X-100 in the presence of hexane. For the system Triton X-100/iso-amyl alcohol/hexane/water, no visible change was observed at neutral pH to pH 6. However, at pH 3, a decrease in the microemulsion zone was observed. The non-ionic surfactants have particular characteristics; they are chemically compatible with most other surfactants and their properties are little affected by pH. It was observed that the decrease in the pH becomes less efficient at forming a microemulsion for the three surfactants. This occurred because with the increasing H^+ ion concentration in the mixture, as in the case of salinity, this ion becomes a competitor with the co-surfactant and surfactants in the water solubility. However, the impact in the microemulsion domain was not as great as in the case of the addition of NaCl because the H^+ can also ionize the surfactants, increasing their solubility. Consequently, as the pH lowers, the H^+ ion interacts less with the surface-active agents and begins to compete with them by solubility.
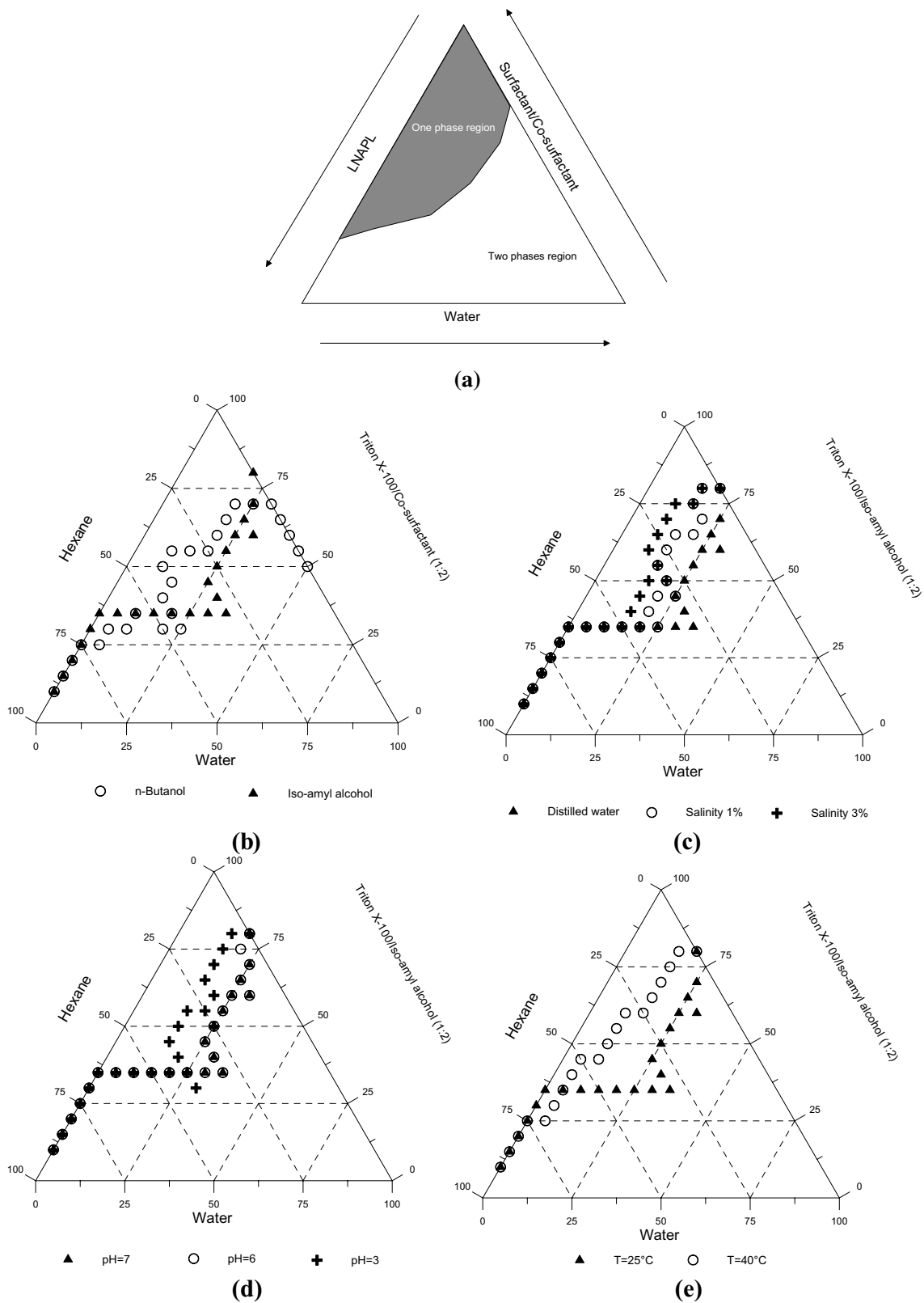
Fig. 4 Pseudo-ternary phase diagrams for the systems hexane-water-Triton X-100/alchool, effect on the formation of zone of one phase: **a** Generic pseudo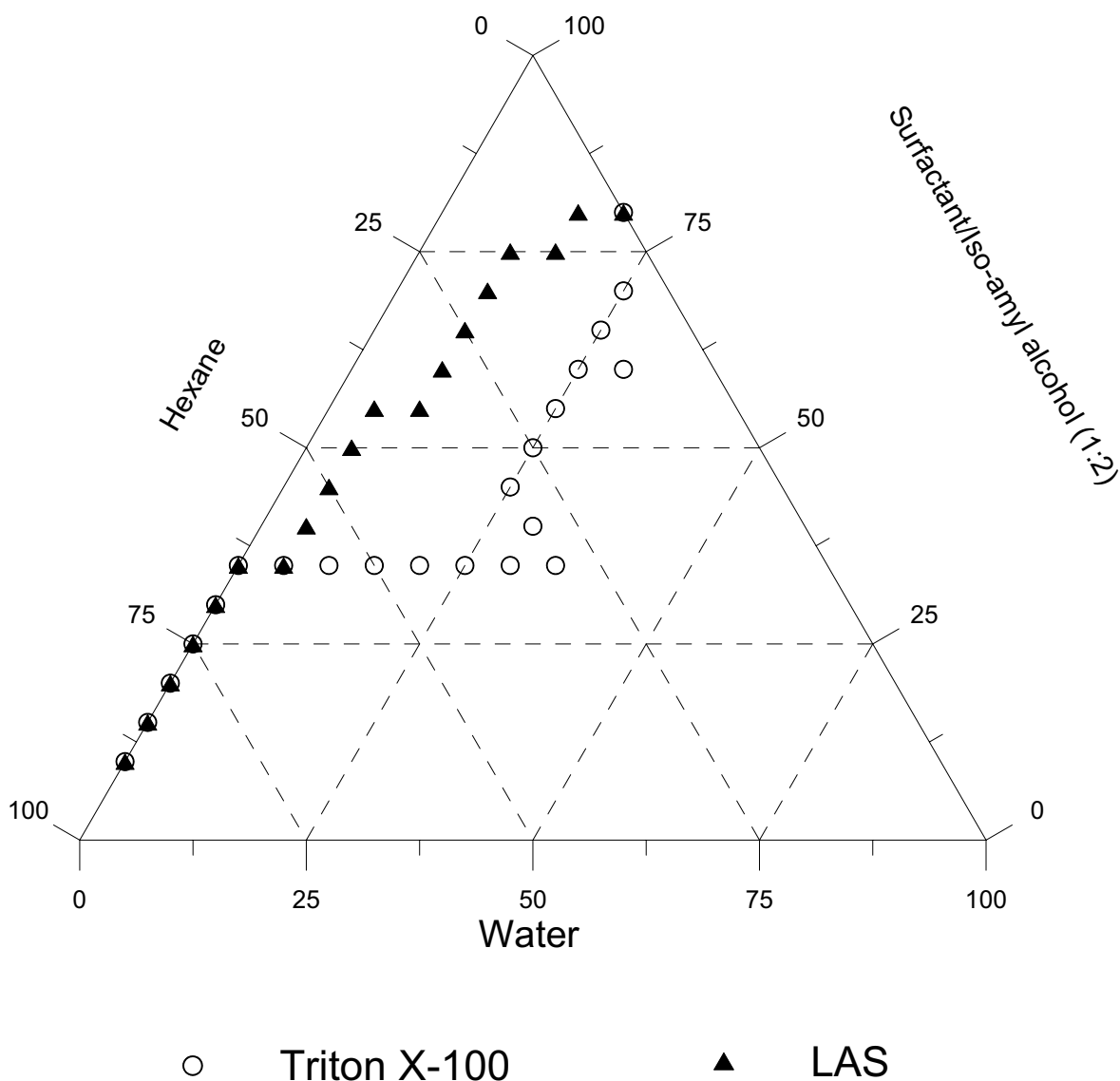-ternary phase diagram showing the zone of one phase (microemulsion); **b** Effect of type of co-surfactant, **c** Effect of the water salinity, **d** Effect of pH, **e** Effect of temperature

Depending on the temperature, the surfactant is more or less soluble in water and oil. The temperature has the opposite effect on ionic and non-ionic surfactants. An increase in temperature causes an increase in the volume of the hydrophobic part of the surfactant, also increasing the solubilization of hydrocarbons in the non-ionic surfactant. In the case of ionic surfactants, increasing temperature increases the solubility of surfactants and water in a microemulsion.

The effect of temperature on the microemulsion domain was studied at 25 and 40 °C. Clearly, the temperature influences the behavior of the microemulsion. In the case of the system hexane/ Triton X-100- iso-amyl alcohol/water, an increase in temperature of 25 to 40 °C causes a decrease in the existence of the microemulsion domain (Fig. 4e).

The increase in temperature weakens the hydrogen bonds of the surfactants, resulting in a decrease in the capacity of solubilization.

The influence of the type of surfactant on the phase behavior was evaluated. Experiments were carried out with Triton X-100 and LAS in the presence of hexane. The phase diagrams (Fig. 5) show a very well-defined microemulsion domain. The diagram shows a net decrease in the domain of one phase when Triton X-100 is replaced with LAS detergent. A two-phase domain is located at the bottom of the diagram for the two surfactants used. This can be explained by the fact that these surfactants have different molecular structures. It was found that the system Triton X-100/hexane/water formed a larger single phase which may be attributed

Fig. 5 Pseudo-ternary phase diagram for the systems hexane-water-surfactant/alcohol, effect of type of surfactant on the formation of zone of one phase

to the larger hydrocarbon chain length of surfactant Triton X-100 compared to the surfactant LAS. Added to this is the fact that Triton X-100 is a non-ionic surfactant, which is an important factor for the stability of microemulsion (Bayrak and Iscan 2005).

There is a decrease in the emulsion capacity of a surfactant with an increase in the hydrocarbon chain length. The microemulsion domain decreases when hexane is replaced by dodecane in the same system and it decreases even more when dodecane is replaced by kerosene (Fig. 6). This decrease can be explained by the fact that the molecules studied here correspond to a succession of identical carbons without the presence of heteroatoms. The number of carbons or the chain length is therefore an important factor in changing the polarity of the molecules. The microemulsion domains are reduced as the carbon chain length increases, which makes kerosene recovery less important than the recovery of hexane. Hexane gives the largest single-phase domain for the Triton X-100/iso-amyl alcohol, LNAPL, and water systems because the Triton X-100 is soluble in short-chain oils, but as the LNAPL compounds chain length increases, the concentration of Triton X-100 in the oil phase decreases.

LNALP microemulsion mobilization

Sandstone core flooding experiments were carried out using kerosene as LNAPL and solutions of Triton X-100/iso-amyl alcohol as a surfactant/co-surfactant and LAS/iso-amyl alcohol as a surfactant/co-surfactant.

Before the flood tests, the properties of the porous bed were determined. The porous media geometry and measurement of water holdup indicate that the volume of voids (V_w) in the core is 11.0 cm^3 and the total volume of the core (V_t) is 226.8 cm^3. Using Eq. 1, the porosity of the bed (ε) can be estimated at 4.85%. The permeability test, for water flow rate variation of 2 to 10 mL/min is summarized in Fig. 7. The flow is according to Darcy's law. The slope of the water flux versus the pressure gradient is 1.4605×10^{-10} m^2/Pa.s, which gives an absolute permeability of 0.13 μm^2 (or 132 mD). The values of porosity and permeability are compatible with fine-textured sandstones, such as the Botucatu Formation, that of the sample used in this study (Kameda 2005; Correa et al. 2019).

The results of the pulse tracer tests for the Botucatu sandstone core sample using a passive tracer are presented in Fig. 8a–c. The plots show a characteristic peak in the

Fig. 6 Pseudo-ternary phase diagram for the systems alkane-water-Triton X-100/alchool, effect of the alkane chain length on the formation of zone of one phase
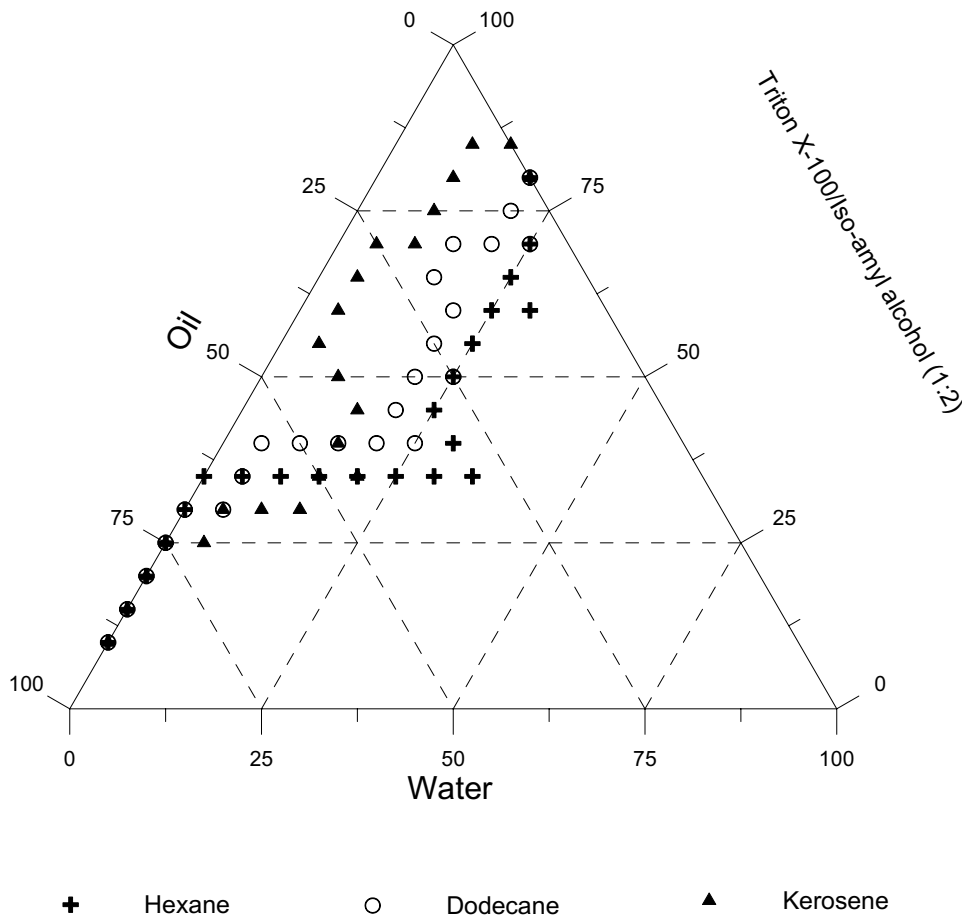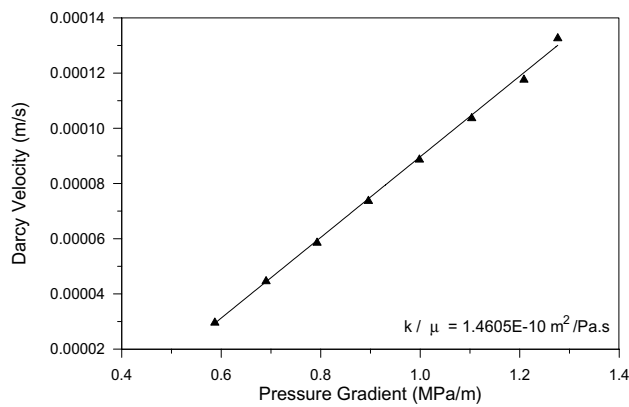
**Fig. 7** Permeability test results for sandstone core ($L = 20.0$ cm and $D = 3.8$ cm)

tracer concentration, an axial dispersion component, and a tail, which indicates some interaction with the solid or the residual liquid phase. These results indicate that the sandstone core sample has a homogeneous internal pore structure because the residence time distribution curves present a regular shape without any by-pass or dead volume, which would be shown by small peaks at the beginning of the curve or a long tail, respectively.

The contrast between Fig. 8a and b indicates a more significant interaction of the tracer with the residual liquid phase (Figs. 8a), which results in a longer tail and strong asymmetric behavior (de Andrade Lima 2006). The tracer concentration peak was observed at 20 and 12 min for a water flow rate of 2.75 and 4.4 mL/min, respectively. Although the time to complete tracer elimination is about 4 h for a flow rate of 2.75 mL/min and about 2 h for a flow rate of 4.4 mL/min, most of the tracers are eliminated in 1 h in both cases (Fig. 8b and c).

The results for the residence time distribution of the Botucatu sandstone core with residual NALP (Fig. 8a) are fitted using the piston-dispersion-exchange model (Fig. 9a) (de Andrade Lima 2006). The result is presented in Fig. 9b. It can be seen that the fit describes the non-ideal flow in the core sample well and this supports the hypothesis of porous media flow with small axial dispersion and interaction with a stagnant zone.

Having defined the properties of the porous bed, the recovery tests of the residual LNAPL started. The purpose of these displacement experiments is to test the efficiency of the chemicals in the recovery of residual LNAPL. The experimental conditions for the screening by core floods are simplified as much as possible.

The oil recovery by a surfactant solution was performed on the porous bed initially saturated with kerosene. Figure 10a shows the recovery of kerosene by mechanical displacement by distilled water followed by the recovery
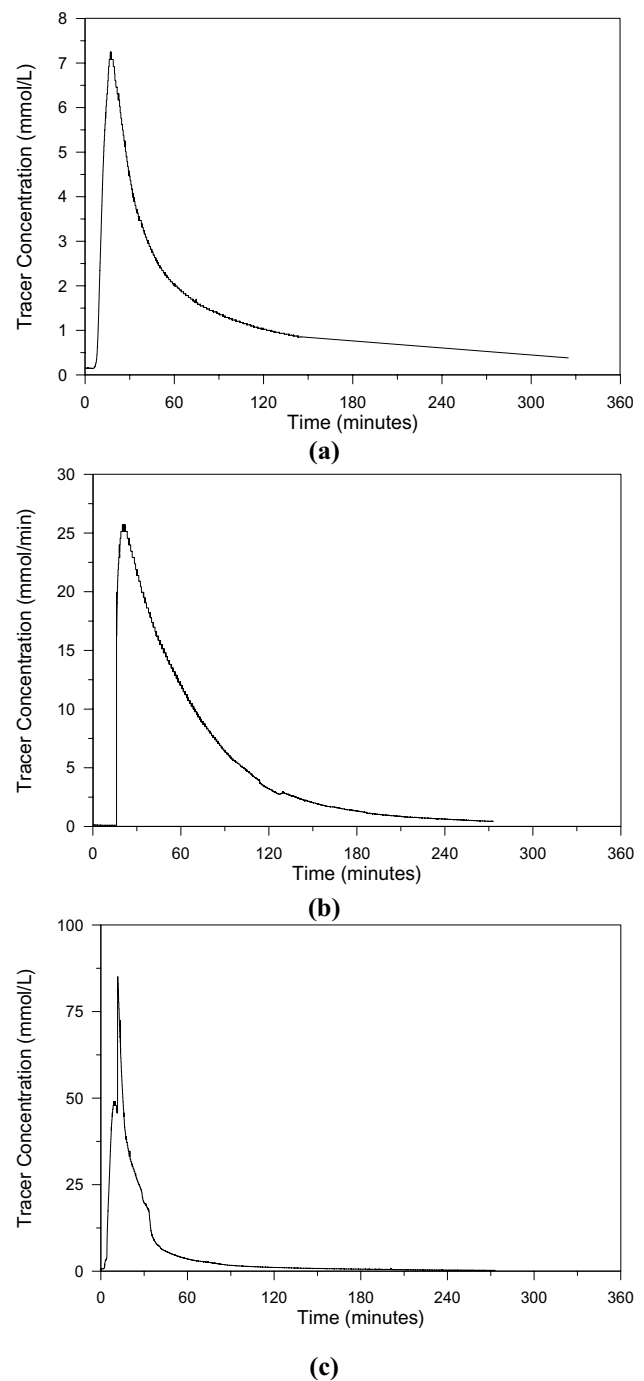
Fig. 8 Tracer tests carried out on Botucatu sandstone core samples for different water flow rates: **a** 2.75 mL/min (with residual NALP in the core pores), **b** 2.75 mL/min, and **c** 4.40 mL/min

using the microemulsion at low concentration of surfactants (Triton X-100 or LAS). The initial recovery in both cases is about 45%. After three bed volumes, the conventional method can no longer recover the residual LNAPL requiring the use of another method. The injection of 7 bed volumes of water resulted in a very low recovery. The injection of 7

Fig. 9 **a** Schematic representation of the PDF model: L is the bed length, C_d is the concentration of the tracer in the dynamic zone, C_s is the concentration of the tracer in the stagnant zone, u_d is the superficial velocity of the solution in the dynamic zone, and $k_m a$ is the mass-transfer coefficient at the interface dynamic-static phase. **b** Model fit for the residence time distribution results of 2.75 mL/min with residual NALP in the core pores (Fig. 8a)
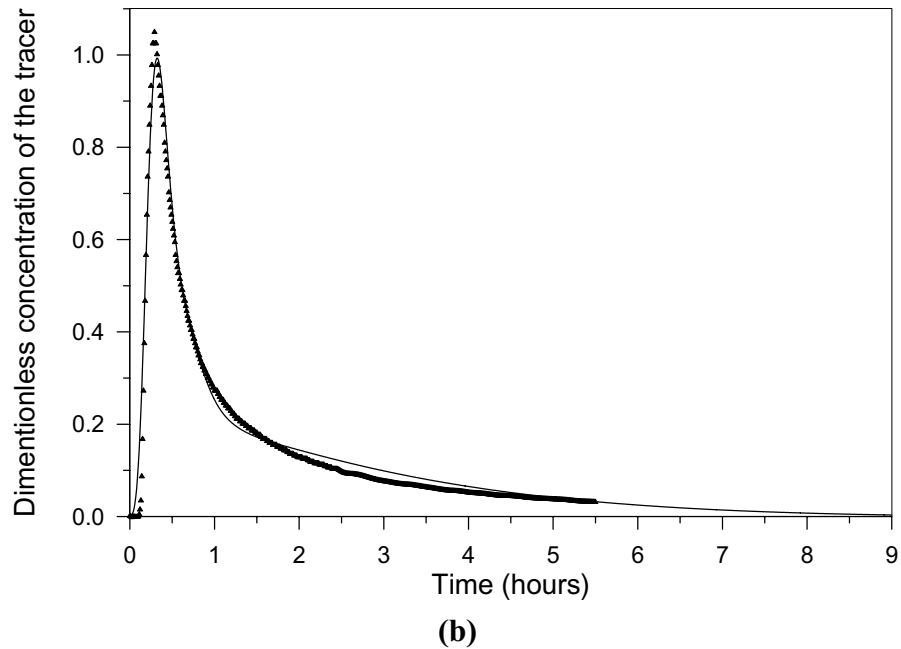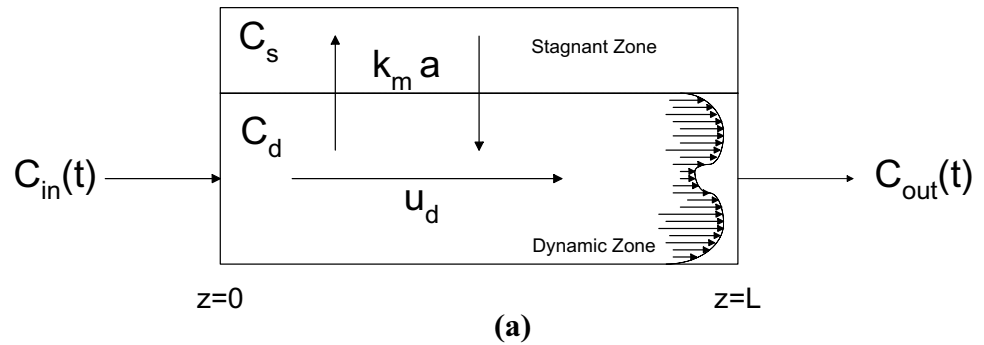

bed volumes of surfactant-co-surfactant mixture/water led to the recovery of 60% for LAS and 50% for Triton X-100. Table 1 shows that the interfacial tension for the system LNAPL/Water using LAS and iso-amyl alcohol is smaller than the interfacial tension for the system LNAPL/Water using Triton X-100 and iso-amyl alcohol, which can explain this result. Previous results in the literature show that the non-ionic surfactants tend to be strongly adsorbed to porous medium, such as shale and sandstone, while anionic surfactant showed minor adsorption affinities to both shale and sandstone (Muherei et al. 2009).

Figure 10b shows the recovery by distilled water followed by the recovery using the microemulsion at a high concentration of surfactant (LAS). The initial recovery is 61%. After two bed volumes, the conventional method can no longer recover the residual LNAPL requiring the use of another method. The injection of 3 bed volumes of water recovered 64%, increasing the recovery of kerosene at the end of the secondary recovery phase to 67%. The injection of 2 bed volumes of surfactant-co-surfactant mixture/water

led to the recovery of 97%, and the total recovery after 3 bed volumes of surfactant-co-surfactant mixture/water was 100%.

Conclusion

The formation of microemulsion in the LNAPL/water/surfactant/co-surfactant system, using hexane and kerosene, Triton X-100, and iso-amyl alcohol and n-butanol was analyzed. The phase diagrams indicate the microemulsion formation domain in a wide zone of low-to-intermediary oil-phase content and high surfactant/co-surfactant content. This one-phase domain was applied to porous bed flooding experiments performed with residual LNAPL saturation (kerosene) in a sandstone core sample using a microemulsion composed of Triton X-100 or LAS and co-surfactant iso-amyl alcohol. The results show the strong effect of the microemulsions in the mobilization of the LNAPL from an aquifer rock using an appropriate formulation of surfactant
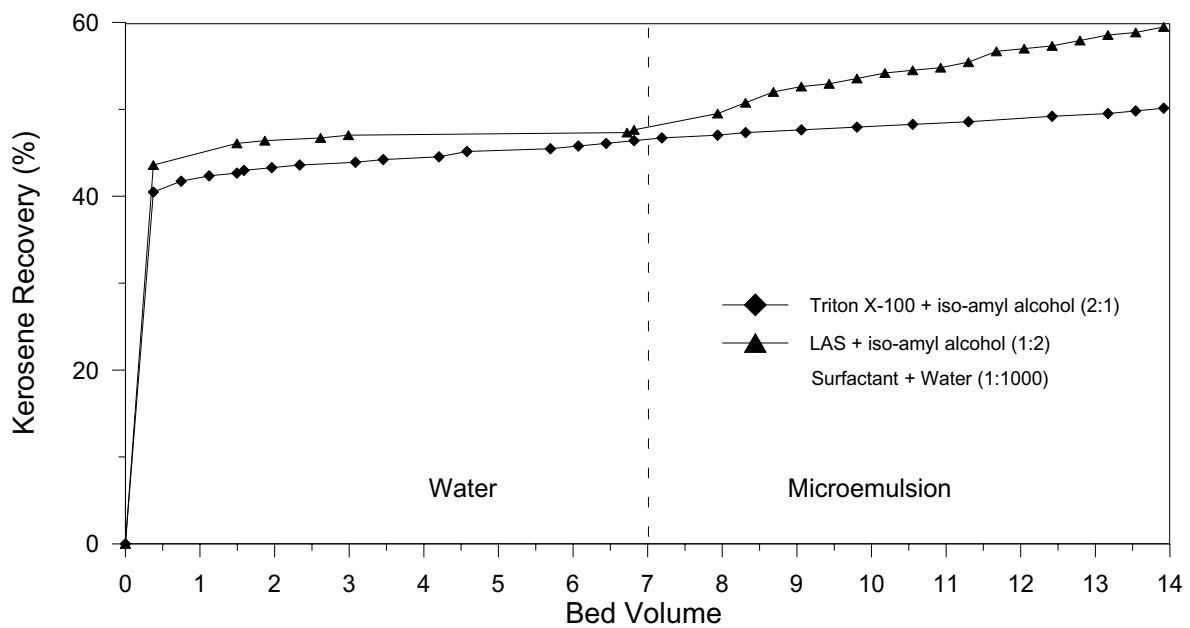
(a)
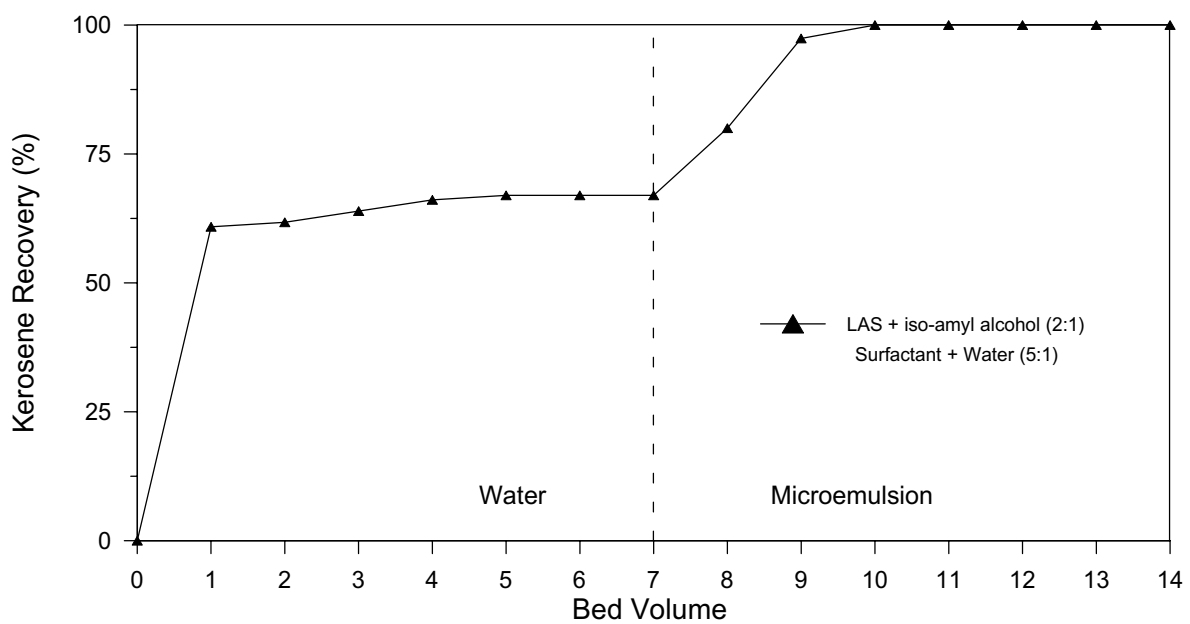
(b)

Fig. 10 Kerosene recovered from sandstone core using pure water and microemulsion injection. **a** Triton X-100/LAS–iso-amyl alcohol at low concentration. **b** LAS—iso-amyl alcohol at high concentration

solutions, the compositions of which were optimized using phase diagrams. Our findings point to the importance of considering the physio-chemical properties of the porous medium and the cost and type of surfactant when selecting microemulsion formulation for removal of LNAPL from porous medium. The results suggest that, despite the

fact the phase diagram studies demonstrate that the system containing surfactant Triton X-100 is more effective in the formation of a microemulsion, the use of ionic sulfonate surfactant LAS in the flooding experiments resulted in an effective recovery, probably due to its structure and ionic characteristic and adsorption properties. Although Triton

X-100 is widely used for remediation, it is more expensive than LAS. In the present case, total recovery of 67% of the LNAPL by water injection was found and 100% recovery (an extra 36%) was found using a high concentration of surfactant/co-surfactant solution injection. The results of this study provide information that can be used for a preliminary feasibility study regarding the use of these surfactants in remediation of LNAPL.

References

Azira H, Tazerouti A (2007) Micellar behaviour of anionic surfactants with sulfonate function in aqueous solutions. J Surf Deterg 10:185–190

Azira H, Tazerouti A, Canselier JP (2008) Phase behaviour of pseudoternary brine: alkane/alcohol-secondary alkanesulfonates systems. Surfactant ratio effects of salinity and alcohol. J Therm Anal Calorim 92:759–763

Bayrak Y, Iscan M (2005) Studies on the phase behavior o f the system non-ionic surfactant/alcohol/alkane/H2O. Colloids Surf A 268:99–103

Bellocq AM, Biais J, Clin B, Gelot A, Lalanne P, Lemanceau B (1980) Three-dimensional phase diagram of the brine-toluene-butanol-sodium dodecyl sulfate system. J Colloid Interface Sci 74:311–321

Bera A, Mandal A (2014) Microemulsions: a novel approach to enhance oil recovery: a review. J Pet Explor Prod Technol 5:255–268

Bernardez LA, de Andrade Lima LRP (2014) Micellar solution to recovery diesel in sand. In: Fanun M (ed) The role of colloidal systems in environmental protection. Elsevier, Amsterdam, pp 453–477

Bernardez LA, de Andrade Lima LRP, Almeida PF (2008) The hydrodynamics of an upflow packed-bed bioreactor at low Reynolds number. Braz J Pet Gas 2:114–121

Bernardez LA, Therrien R, Lefebvre R, Martel R (2009) Simulating the injection of micellar solutions to recover diesel in a sand column. J Contam Hydrol 103:99–108

Bigarella JJ, Salamuni R (1967) The Botucatu formation. In: Bigarella JJ, Becker RD, Pinto JD (eds) Problems in Brazilian Gondwana geology. UFPR, Curitiba, pp 198–206

Ceglie A, Das KP, Lindman B (1987) Effect of the chain length of oil on the systems for different surfactants. Colloids Surf 28:29–40

Correa JC, Garcia RHL, dos Santos RS, Amadeu RA, Bernardes TLS, Velo AF, Carvalho DVS, do Nascimento TJ, Cavallaro FA, de Mesquita CH, Hamada MM (2019) Chemical and physical analysis of sandstone rock from Botucatu formation, International Nuclear Atlantic Conference-INAC 2019, Santos, SP, Brazil.

de Andrade Lima LRP (2006) Liquid axial dispersion and holdup in column leaching. Miner Eng 19:37–47

Demirbas A, Alsulami HE, Hassanein WS (2015) Utilization of surfactant flooding processes for enhanced oil recovery (EOR). Pet Sci Technol 33:1331–1339

Huh C, Mason SG (1975) A rigorous theory of ring tensiometry. Colloid Polym Sci 253:566–580

Iglauera S, Wu Y, Shulera P, Tanga Y, Goddard WA (2009) Alkyl polyglycoside surfactant–alcohol cosolvent formulations for improved oil recovery . Colloids Surf A 339:48–59

Javanbakht G, Goual L (2016) Mobilization and micellar solubilization of NAPL contaminants in aquifer rocks. J Contam Hydrol 185–186:61–73

Javanbakht G, Arshadi M, Qin T, Goual L (2017) Micro-scale displacement of NAPL by surfactant and microemulsion in heterogeneous porous media. Adv Water Resour 105:173–187

Jeirani Z, Mohamed Jan B, Si Ali B, See CH, Saphanuchart W (2014) Pre-prepared microemulsion flooding in enhanced oil recovery: a review. Pet Sci Technol 32:180–193

Jin F-Y, Wang S, Pu W-F, Liu X-L, Yuan C-D, Zhao S, Tang Y-L, Dou L (2016) The effects of interfacial tension, injection rate, and permeability on oil recovery in dilute surfactant flooding. Pet Sci Technol 34:1490–1495

Kahlweit M, Strey R, Busse G (1991) Effect of alcohols on the phase behavior of microemulsions. J Phys Chem 95(13):5344–5352

Kameda A (2005) Permeability evolution in sandstone: digital rock approach, PhD Thesis in Geophysics, Stanford University.

Kegel WK, Lekkerkerker HNW (1993) Phase behaviour of an ionic microemulsion system as a function of the co-surfactant chain length. Colloids Surf A 76:241–248

Li H, Chen J, Yang J (2011) Pore-scale removal mechanisms of residual light non-aqueous phase liquids in porous media. Environ Earth Sci 64:2223–2228

Li H, Chen J, Jiang L (2014) Elevated critical micelle concentration in soil–water system and its implication on PAH removal and surfactant selecting. Environ Earth Sci 71:3991–3998

Martel R, Gélinas PJ, Desnoyers JE (1993) A. Masson, Phase diagrams to optimize surfactant solutions for oil and DNAPL recovery in aquifers. Gr Water 31:789–800

Muherei M, Junin R, Merdhah AB (2009) Adsorption of sodium dodecyl sulfate, Triton X-100 and their mixtures to shale and sandstone: a comparative study. J Pet Sci Eng 67(3):149–154

Salager JL, Morgan JC, Schechter RS, Wade WH, Vasquez E (1979) Optimum formulation of surfactant/water/oil systems for minimum interfacial tension or phase behavior. SPEJ 19:107–115

Sanz CA, Pope GA (1995) Alcohol-Free Chemical Flooding: From Surfactant Screening to Coreflood Design. In: Proceedings of the SPE International Symposium on Oilfield Chemistry, San Antonio, TX, February, pp 14–17

Voca BR, Canselier JP, Nok C, Bavire M (1988) Three-phase behavior of brine/alkane/alcohol/alpha-olefinsulfonate mixtures. Progr Colloid Polym Sci 76:144–152

Xu J, Li G, Zhang Z, Zhou G, Ji K (2001) A study of the microstructure of CTAB/1-butanol/octane/water system by PGSE-NMR, conductivity and cryo-TEM. Colloids Surf A 191:269–278